

# Large-Scale Dynamic Ridesharing with Iterative Assignment

Akhil Vakayil<sup>1,2</sup>, Felipe de Souza<sup>1</sup>, Taner Cokyasar<sup>1,3</sup>,  
Krishna Murthy Gurumurthy<sup>1</sup>, and Jeffrey Larson<sup>1</sup>

<sup>1</sup>Argonne National Laboratory, 9700 S. Cass Ave., Lemont, IL 60439, USA

<sup>2</sup>Georgia Institute of Technology, North Ave. NW, Atlanta, GA 30332, USA

<sup>3</sup>TrOpt R&D, Balcali mah., Saricam, 01330, Adana, Turkey

November 13, 2023

## Abstract

Transportation network companies (TNCs) have become a highly utilized transportation mode over the past years. At their emergence, TNCs were serving ride requests one by one. However, the economic and environmental benefits of ridesharing encourages them to dynamically pool multiple ride requests to enable people to share vehicles. In a dynamic ridesharing (DRS) system, a fleet operator seeks to minimize the overall travel cost while a rider desires to experience a faster (and cheaper) service. While the DRS may provide relatively cheaper trips by pooling requests, the service speed is contingent on the objective of the vehicle-to-rider assignments. Moreover, the operator must quickly assign a vehicle to requests to prevent customer loss. In this study we develop an iterative assignment (IA) algorithm with a balanced objective to conduct assignments quickly. A greedy algorithm from the literature is also tailored to further reduce the computational time. The IA was used to measure the impact on service quality of fleet size; assignment frequency; the weight control parameter of the two objectives on vehicle occupancy—rider wait time and vehicle hours traveled. A case study in Austin, TX, reveals that the key performance metrics are the most sensitive to the weight parameter in the objective function.

**Keywords:** Large-scale ridesharing, operator- and customer-centric ridesharing, optimization

## 1 Introduction

Ridesharing commonly refers to two or more simultaneous trips being carried out in a single vehicle. This increase in vehicle occupancy is often encouraged to reduce the number of vehicles on roads (Morency, 2007). Apart from reducing traffic congestion, ridesharing can also decrease costs for both customers and vehicle operators. Hence, transportation network companies (TNCs) offer pooling options, such as Uber Pool and Lyft Line (Lawler, 2014). A recent survey reveals that a large majority of riders prefer these pooled services to their single-ride counterparts because they are “cheaper” and “better for the environment” (Sarriera et al., 2017). To maximize these benefits, it is essential to have a system-level vehicle-to-rider matching approach that optimizes certain objectives, such as minimizing total travel time or delay time.

In a dynamic ridesharing (DRS) environment, customers make ride requests through their smartphones, and the TNC operator must *quickly* assign these requests to vehicles that are either idle or currently serving other requests but with available seats (Agatz et al., 2011). These assignments must respect a predefined maximum time within which a rider has to be picked up, as well as the maximum allowed rerouting delay for each rider currently being served. Pick-up and drop-off concerns constrain the TNC operator’s possible assignment combinations. (If a request is not promptly served, customers may reconsider an alternative transportation mode.) In large-scale transportation networks, assigning requests to vehicles quickly while accounting for operator and rider benefits is burdensome; the main motivation in this study is to address such limitations. Although making assignments in real time may be a simple approach, a batched assignment approach in which rider-to-vehicle assignments are carried out at predetermined time intervals can be potentially more beneficial to both TNC operators and riders. The reason is that batching may enable greater coordination of pick-ups and drop-offs.

In this study we propose an iterative assignment IA algorithm to assign rider requests to TNC vehicles at discrete time intervals. In each batching interval, we solve linear programs (LPs) iteratively to minimize two objectives: total TNC fleet travel time and total customer delay time. The first objective approaches the problem from a fleet operator standpoint; the second objective considers a customer-centric assignment. This approach eliminates the need to solve integer programs (IPs), which are often more time-consuming to solve compared with their linear programming relaxations. Apart from the IA algorithm, we tailor a greedy real-time algorithm that assigns requests to vehicles as soon as they emerge in the communication network (Gurumurthy et al., 2020). The greedy algorithm has a considerably shorter time-to-solution and serves as a benchmark to the IA. Our numerical tests focus on key parameters, including the time required to solve each problem, TNC fleet size, the number of vehicles considered for a given request, the trade-off in the objective between customer-centric and operator-oriented approaches, and the batching interval duration. We provide detailed analysis to highlight the impact of these parameters on essential solution metrics, namely, vehicle occupancy and response time.

Both the IA and the greedy approaches have been implemented as components of POLARIS, the Planning and Operations Language for Agent-based Regional Integrated Simulation (Auld et al., 2016) software. POLARIS is an agent-based simulation tool developed by Argonne National Laboratory’s Vehicle and Mobility Systems Department and is used to quantify the impact of emerging and existing vehicle and transportation technologies on a variety of metrics, such as vehicle miles traveled, energy consumed, and greenhouse gas emitted in large metropolitan areas. Time-to-solution becomes a vital determinant of the methodology derivation process because the study is devoted to large-scale DRS, and the solution time of this approach should not pose a bottleneck in the POLARIS tool.

The outline of the manuscript is as follows. Section 2 provides a thorough literature review while comparing the solution approaches. Section 3 formally describes the problem, assumptions, notations, and solution approaches. Section 4 contains numerical experiments that measure the impact of batching interval and the trade-off between the operator-centric and customer-centric perspectives. We also study the effect of fleet size on key solution metrics and the impact of number of vehicles considered for each request in large-scale computational experiments. Section 5 summarizes the work and displays the future of the problem from our perspective.

## 2 Literature Review

DRS is a well-studied subject in the transportation literature, and several review articles have summarized existing works (Furuhata et al., 2013; Martins et al., 2021; Tafreshian et al., 2020; Tahmasseby et al., 2014). DRS is expected to reduce traffic congestion by increasing vehicle occupancy. Alisoltani et al. (2021) used a simulation to assess the validity of this perception and found that the DRS can be impactful in large-scale transportation networks, whereas its contribution is slight in small- and medium-scale networks. Alonso-Mora et al. (2017) demonstrated a multistep approach to tackle the DRS problem where they first construct a pairwise shareability graph, apply pruning to create a candidate trip’s graph, and optimize over the graph using an IP. Their solution methodology is shown to efficiently match over 800,000 riders with 3,000 vehicles, and they report an average of 2,000 riders in each of their IPs solved. A major difference in our study is that the IA is capable of assigning more than one rider to a vehicle at each iteration, whereas their model assigns only one rider to each vehicle.

Agatz et al. (2012) listed three common objectives in ridesharing optimization models: (i) minimize total vehicle miles traveled, (ii) minimize total vehicle times traveled, and (iii) maximize the number of vehicle-to-rider matches. In this study we minimize the cost incurred by the service provider and customers for serving all incoming requests. The service provider costs account for the marginal travel cost increase (due to detour) for serving a given request. The experienced customer cost is the excess time traveled to reach its destination compared with a direct trip from its origin to its destination. Furuhata et al. (2013) divided ridesharing patterns into four classes based on spatiotemporal information of riders: identical, inclusive, partial, and detour. Here, identical refers to the same origin and destination (OD) pairs as well as time schedules for two riders; inclusive means one rider’s OD pair is spanned by another rider’s OD pair while time schedules allow such sequential pick-up/drop-off ordering; partial refers to the case in which one rider’s either origin or destination is different from another but time schedules allow shared service; detour represents the scenario in which OD pairs for riders are distinct but time schedules allow shared service. The solution methodologies proposed in this study consider all of these patterns.

*Path flexibility* allows amending the current vehicle route to pick up a rider. *Multi-hop* refers to transferring a rider from one vehicle to another to gain improvement in the objective. Masoud and Jayakrishnan (2017b) categorized the ridesharing studies in the literature based on the flexibility of paths, multi-hop routes, the ability to handle multiple riders, the solution algorithm, and the optimality of the solution. We account for path flexibility and both individual and grouped riders, for example, a group of friends with common OD pairs. We do not account for the multi-hop and find it an approach that may potentially make riders uncomfortable. We propose both an optimization model finding an optimal solution in a given batching interval and a greedy heuristic to solve the problem. However, these methodologies provide proxies since large-scale problems are considered, and finding the globally optimal solution for an entire day in such problems is difficult if not impossible.

Masoud and Jayakrishnan (2017b) stated that many studies considered the rolling horizon approach in which the TNC operator solves a static ridesharing problem at discrete time intervals as requests are batched. Agatz et al. (2012) mentioned that solving these problems can become challenging in large-scale transportation networks as the computational complexity quickly increases. To address this situation, researchers have used decomposition, partitioning, and clustering methods (Agatz et al., 2012; Masoud and Jayakrishnan, 2017a; Najmi et al., 2017; Nourinejad and Roorda, 2016; Pelzer et al., 2015; Shen et al., 2016). It is known that such partitioning methods

may eliminate potential better assignments, and minimizing the optimality loss requires solving an NP-hard min-cut problem (Aissi et al., 2008; Johnson et al., 1993). In this study we limit the number of vehicles queried for each request to control the problem complexity. We note that such an approach may also end up missing better vehicle-to-rider assignments. However, this limit can be easily tuned to balance the trade-off between the computational time and the solution quality.

### 3 Methodology

In this section we provide notation, state the problem formally, present an assignment problem with its relaxation, propose the IA algorithm, address the possible infeasibility of the LP, shed light on the operator- and customer-centric objectives, and propose a greedy real-time assignment approach.

#### 3.1 Notation and formal problem statement

Given a set of available vehicles  $\mathcal{V}$ , let  $\mathcal{R}$  be the set of customer requests that arrive between the start and end of our planning window. The duration of this batching window is denoted by  $B$ . A request denotes one or more riders scheduling a trip between two locations. Let  $Q_r$  be the number of people to be served in request  $r$ , and let  $\bar{Q}_v$  be the number of available seats in vehicle  $v$ . Each request  $r$  has an expected travel time without ridesharing,  $T_r$ . Compared with an immediate assignment approach in which a request is assigned to a vehicle as soon as one is available, batching requests allows for matchings that are potentially better (for both the passengers’ wait times and drivers’ travel times).

In a large-scale dynamic ridesharing problem, however, considering all available vehicles as candidates for serving every request  $r \in \mathcal{R}$  can be computationally expensive. Thus, we denote  $\mathcal{V}_r$  as a subset of vehicles that can be matched with a given  $r \in \mathcal{R}$ . While many possible approaches for forming  $\mathcal{V}_r$  exist, we let  $\mathcal{V}_r$  contain the  $N$  vehicles closest to the origin location of  $r$  that have space available to accommodate  $r$ . This set can be efficiently queried from the transportation network by using a  $k$ - $d$ -tree-based nearest-neighbor search.

Let  $T_{rv}$  be the travel cost of assigning request  $r$  to vehicle  $v$ . If  $v$  is idle,  $T_{rv}$  is the total duration  $v$  has to travel to pick up and drop off  $r$ . Otherwise,  $T_{rv}$  is the additional duration  $v$  has to travel to include  $r$  in its route plan. The route plan of a vehicle provides the order in which pick-ups and drop-offs are executed by the vehicle for the requests being served by it. Let  $\Theta_v^0$  be the existing route plan of vehicle  $v$ , wherein  $v$  could be already catering to one or more requests, and let  $\Theta_v^r$  be the potential route plan where  $v$  accommodates  $r$ . Then  $T_{rv}$  is computed as the excess travel time on route plan  $\Theta_v^r$  compared with  $\Theta_v^0$ . Ideally, the route plans are to be determined by computing constrained shortest paths, an expensive affair that we circumvent by heuristically predetermining the pick-up and drop-off order based on Euclidean or Manhattan distance. In other words, starting from the current vehicle location, the next pick-up or drop-off location is chosen based on its closeness to the vehicle’s previous location, all the while making checks that the drop-off for a request can happen only if its corresponding pick-up has already occurred.

We let  $D^P$  denote the maximum allowed pick-up delay for all requests. If a request is not satisfied within  $D^P$  time units of when it was made, then the request is left to find an alternative transportation mode (e.g., bus, rail, or an individually owned car). Let  $D_r^T$  be the maximum

allowed travel delay for request  $r$ ; this will be set by

$$D_r^T := \max\{\bar{D}, T_r \times D^\%\}, \quad (1)$$

where  $\bar{D}$  is a fixed minimum value for the travel delay threshold, say 10 minutes, and  $D^\%$  is a threshold as a percentage of the expected travel time. For example, if  $D^\%$  is 0.33, a maximum of  $\approx 20$  minutes travel delay is allowed for a request with an expected travel time of 1 hour. [Table 1](#) details the sets, parameters, and decision variables to be used throughout.

Table 1: Sets, parameters, and variables describing the ridesharing problem

Set	Definition
$\mathcal{R}$	Set of requests in the batching period.
$\mathcal{V}_r$	Subset of vehicles that can potentially service request $r$ .
$\mathcal{V}$	Set of vehicles that can be assigned in the batching period, $\mathcal{V} = \cup_{r \in \mathcal{R}} \mathcal{V}_r$ .
$\mathcal{E}$	Set of edges $(r, v)$ such that $r \in \mathcal{R}, v \in \mathcal{V}_r$ .
Parameter	Definition
$B$	Batching period duration.
$T_r$	Expected travel time without ridesharing for request $r$ , $\forall r \in \mathcal{R}$ .
$N$	Number of potential vehicles to consider in $\mathcal{V}^r$ , $\forall r \in \mathcal{R}$ .
$D^P$	Maximum allowed pick-up delay for any request.
$D_r^T$	Maximum allowed travel delay for request $r$ , $\forall r \in \mathcal{R}$ .
$Q_r$	Number of customers requesting a ride in request $r$ , $\forall r \in \mathcal{R}$ .
$\bar{Q}_v$	Seats available in vehicle $v$ , $\forall v \in \mathcal{V}$ .
$\Theta_v^0$	The route plan followed by vehicle $v$ before making assignments in the current batch, $\forall v \in \mathcal{V}$ .
$\Theta_v^r$	The potential route plan of vehicle $v$ if $v$ has to accommodate request $r$ , $\forall (r, v) \in \mathcal{E}$ .
$T_{rv}$	Additional duration vehicle $v$ would have to travel to serve request $r$ , that is, the difference in travel time on route plan $\Theta_v^r$ and $\Theta_v^0$ , $\forall (r, v) \in \mathcal{E}$ .
Variable	Definition
$x_{rv}$	1 if request $r$ is assigned to vehicle $v$ , $\forall (r, v) \in \mathcal{E}$ , 0 otherwise

### 3.2 Assignment problem and relaxation

Matching requests to vehicles can be viewed as an assignment problem constrained by vehicle capacities. Two setbacks can arise when modeling the ridesharing problem in a large-scale transportation network as an assignment problem: (i) solving a large integer program at the end of every batching period can become a computational bottleneck, and (ii) the cost of assigning a request to a vehicle depends on the set of requests assigned to this vehicle in the same batching period. This cost dependence does not appear in traditional assignment problems. We propose the IA process, motivated by the iterative approximation algorithm for the generalized assignment problem in [Lau et al. \(2011\)](#), to address both of these concerns.

Assignment problems can be solved by forming a bipartite graph. In our case we let  $G = (\mathcal{R} \cup \mathcal{V}, \mathcal{E})$ , where  $\mathcal{V} = \cup_{r \in \mathcal{R}} \mathcal{V}_r$  is the set of vehicles considered in the batch and  $\mathcal{E} = \{(r, v) : r \in \mathcal{R}, v \in \mathcal{V}_r\}$  is the set of edges in  $G$ . Binary variables  $x_{rv} \in \{0, 1\}, \forall (r, v) \in \mathcal{E}$  will be used to denote whether request  $r$  is assigned to vehicle  $v$  in the integer program. We let  $\text{LP}(G)$  be the linear relaxation (allowing for fractional values for  $x_{rv}$ ) of this integer linear assignment program on  $G$ , namely,

$$\text{LP}(G) := \begin{cases} \text{minimize}_{x_{rv}} & \sum_{(r,v) \in \mathcal{E}} T_{rv} x_{rv} & (2) \\ \text{subject to} & \sum_{v:(r,v) \in \mathcal{E}} x_{rv} = 1, \forall r \in \mathcal{R} & (3) \\ & \sum_{r:(r,v) \in \mathcal{E}} Q_r x_{rv} \leq \bar{Q}_v, \forall v \in \mathcal{V} & (4) \\ & x_{rv} \geq 0, \forall (r,v) \in \mathcal{E}, & (5) \end{cases}$$

where the objective function (2) minimizes the total additional duration vehicles need to travel to serve their corresponding requests; constraints (3), which we will denote as  $\mathcal{C}_{\mathcal{R}}$ , impose that every request should be matched to only one vehicle (if  $x_{rv} \in \{0, 1\}, \forall (r, v) \in \mathcal{E}$ ); constraints (4), which we will denote as  $\mathcal{C}_{\mathcal{V}}$ , ensure that vehicle capacities are not exceeded; constraints (5) are the non-negativity constraints.

### 3.3 Iterative assignment algorithm

We can solve one or more linear programs at the end of every batching period instead of one large-scale integer program, provided the size of the linear programs is reduced over successive iterations. Algorithm 1 presents the IA algorithm that attempts to do the same. Given an initial set of requests  $\mathcal{R}^0$  and vehicles  $\mathcal{V}^0$  resulting in the bipartite graph  $G^0$ , the IA proceeds by removing infeasible variables (edges) in  $G^0$ ; that is, variable  $x_{rv}$  is removed if the number of people requesting a ride in request  $r$  exceeds the number of seats available in vehicle  $v$  or if serving  $r$  increases the pick-up or travel delay of any of the customers in  $v$  beyond a threshold as detailed in Section 3.1. After finishing the initial pruning step, if there are no feasible vehicles for a request  $r$ , that is,  $\text{deg}(r) = 0$  in  $G^0$ , then  $r$  cannot be assigned in the current batch and is removed from  $\mathcal{R}^0$ . We will use  $\text{LP}(G)$  to refer to the linear programs being solved within iterations of the IA, as  $\text{LP}(G^0)$  is used to refer to the original linear program, and  $G$  is a subset of  $G^0$  in every iteration. For ease of presentation, we assume in this subsection that each  $\text{LP}(G)$  encountered is feasible. In Section 3.4, we demonstrate what to do when an infeasible instance of  $\text{LP}(G)$  is encountered. Assuming the linear program is feasible, the IA solves  $\text{LP}(G)$  and then makes use of the optimal solution thus obtained to intelligently assign a subset of requests before moving on to the next iteration to address the requests that remain.

We will now explore how to make the assignments after solving  $\text{LP}(G)$  in every iteration of the IA. We could make a request  $r$  to vehicle  $v$  assignment if variable  $x_{rv}$  in the optimal solution takes value 1; but if we end up assigning multiple requests to a single vehicle within the same iteration, the cost of assignment will be incorrect, which was our second concern alluded to in Section 3.2. For example, if two requests  $r^1$  and  $r^2$  are assigned to vehicle  $v$ , the cost of assignment is not equal to  $T_{r^1v} + T_{r^2v}$ . Hence, instead of making all  $r - v$  assignments for which  $x_{rv}$  takes value 1 in the optimal solution, for those vehicles that potentially get multiple requests assigned, we only assign the request with the least cost of assignment (breaking ties arbitrarily); the remaining requests are pushed to the next iteration. For vehicle  $v$  that was assigned a request  $r$ , we update the route plan of  $v$  to reflect the assignment, that is,  $\Theta_v^0 \leftarrow \Theta_v^r$ . Before the IA proceeds to the next iteration, the assignment costs for all the vehicles that were assigned a request in the current iteration are recomputed. For example, if requests  $r^1$  and  $r^2$  were feasible for vehicle  $v$  and if  $r^1$  was assigned

to  $v$  and  $r^2$  remains unassigned in the current iteration, then  $T_{r^2v}$  has to be recomputed if  $v$  is still feasible for  $r^2$ , after updating the existing route plan of  $v$  to reflect the  $r^1 - v$  assignment, that is,  $\Theta_v^0 \leftarrow \Theta_v^{r^1}$ . Doing so maintains the validity of the cost of all assignments within all iterations of the IA. The edges  $(r, v) \in \mathcal{E}$  that become infeasible at the end of an iteration are removed from  $G$ ; and if there are no feasible vehicles for a request  $r$ , that is,  $\deg(r) = 0$  in  $G$ , then  $r$  cannot be assigned a vehicle in the current batch and is removed from  $\mathcal{R}$ . The requests that were initially present in  $\mathcal{R}^0$  and are not assigned a vehicle in the final matching  $\mathcal{M}$  that is returned when [Algorithm 1](#) terminates can return in the next batch if their pick-up-delay threshold permits; otherwise, they are left to find alternative transportation modes.

To show that the IA terminates within a deterministic maximum number of iterations, we make use of [Lemma 1](#). If the optimal extreme point solution of  $\text{LP}(G)$  contains no variable  $x_{rv}$  that takes value 1 in an iteration, [Lemma 1](#) guarantees that if  $\text{LP}(G)$  is feasible, there exists at least one variable that takes a value of 0. In such an iteration of the IA, we remove all edges  $(r, v) \in \mathcal{E}$  for which  $x_{rv}^* = 0$  and then proceed to the next iteration. We have now ensured that with every iteration the problem instance reduces by at least one request (node) or variable (edge), thereby asserting that the IA terminates in a finite number of iterations on the order of size  $G^0$ .

---

**Algorithm 1:** Iterative Assignment (IA)

---

```

1 Inputs:  $\mathcal{R}^0, \mathcal{V}^0, \mathcal{E}^0$ 
2 Remove infeasible edges from  $\mathcal{E}^0$  // Based on capacity and delay thresholds (see Section 3.3 for details)
3  $\mathcal{M} \leftarrow \emptyset$ ;  $\mathcal{R} \leftarrow \mathcal{R}^0$ ;  $\mathcal{V} \leftarrow \mathcal{V}^0$ ;  $\mathcal{E} \leftarrow \mathcal{E}^0$ 
4 while  $\mathcal{E} \neq \emptyset$  do
5    $\mathcal{V}^a \leftarrow \emptyset$  // Set of vehicles that are assigned a request in the current iteration
6   if  $\text{LP}(G)$  is infeasible then
7      $\mathcal{R}, \mathcal{V}, \mathcal{E}, G_U, \mathcal{M} \leftarrow$  Algorithm 2( $\mathcal{R}, \mathcal{V}, \mathcal{E}, \mathcal{M}$ )
8     Solve  $\overline{\text{LP}}(G_U)$  to obtain an optimal extreme point solution  $\mathbf{x}^*$ 
9   else
10    Solve  $\text{LP}(G)$  to obtain an optimal extreme point solution  $\mathbf{x}^*$ 
11   if  $\exists (r, v) \in \mathcal{E} : x_{rv}^* = 1$  then
12     for  $v^0 \in \mathcal{V} : \exists r \in \mathcal{R}$  with  $x_{rv^0}^* = 1$  do
13        $r^0 \leftarrow \arg \min_{r \in \mathcal{R}} \{T_{rv^0} : x_{rv^0}^* = 1\}$ 
14        $\mathcal{M} \leftarrow \mathcal{M} \cup (r^0, v^0)$ ;  $\mathcal{V}^a \leftarrow \mathcal{V}^a \cup \{v^0\}$ ;  $\mathcal{R} \leftarrow \mathcal{R} \setminus \{r^0\}$ ;  $\overline{Q}_{v^0} \leftarrow \overline{Q}_{v^0} - Q_{r^0}$ ;  $\Theta_{v^0}^0 \leftarrow \Theta_{v^0}^0$ 
15        $\mathcal{E} \leftarrow \mathcal{E} \setminus \{(r^0, v) : v \in \mathcal{V}, (r^0, v) \in \mathcal{E}\}$ 
16   else if  $\exists (r, v) \in \mathcal{E} : x_{rv}^* = 0$  then
17      $\mathcal{E} \leftarrow \mathcal{E} \setminus \{(r, v) : x_{rv}^* = 0\}$ 
18   for  $v \in \mathcal{V}^a$  do
19     for  $r \in \mathcal{R} : (r, v) \in \mathcal{E}$  do
20       if edge  $(r, v)$  is infeasible then
21          $\mathcal{E} \leftarrow \mathcal{E} \setminus \{(r, v)\}$ 
22       else
23         Recompute  $T_{rv}$ 
24    $\mathcal{R} \leftarrow \{r \in \mathcal{R} : \deg(r) \neq 0\}$ 
25    $\mathcal{V} \leftarrow \{v \in \mathcal{V} : \deg(v) \neq 0\}$ 
26 return  $\mathcal{M}$ 

```

---

**Lemma 1.** Given  $Q_r \leq \overline{Q}_v$ ,  $\forall (r, v) \in \mathcal{E}$ , let  $\mathbf{x}$  be an extreme point solution of  $\text{LP}(G)$ . Then  $\exists (r, v) \in \mathcal{E} : x_{rv} \in \{0, 1\}$ .

*Proof.* Let us prove by contradiction. Assume there exists some  $\text{LP}(G)$  with extreme point solution

$\mathbf{x}$  such that  $0 < x_{rv} < 1, \forall (r, v) \in \mathcal{E}$ . The constraint set  $\mathcal{C}_{\mathcal{R}}$  tells us that  $\deg(r) \geq 2, \forall r \in \mathcal{R}$  since an all-fractional solution is infeasible for  $\text{LP}(G)$  if there exists a request  $r$  with  $\deg(r) = 1$ . We have that

$$|\mathcal{E}| = \frac{1}{2} \left( \sum_{r \in \mathcal{R}} \deg(r) + \sum_{v \in \mathcal{V}} \deg(v) \right) \geq |\mathcal{R}| + \frac{1}{2} \sum_{v \in \mathcal{V}} \deg(v). \quad (6)$$

Since  $\mathbf{x}$  is an extreme point solution, we know that there are at least  $|\mathcal{E}|$  linearly independent constraints that are active at  $\mathbf{x}$ , that is, satisfied as equality. Let us now partition  $\mathcal{V}$  into two groups  $\mathcal{V}^\alpha$  and  $\mathcal{V}^\beta$  such that  $\deg(v) = 1, \forall v \in \mathcal{V}^\alpha$  and  $\deg(v) \geq 2, \forall v \in \mathcal{V}^\beta$ . Also, let  $|\mathcal{V}^\alpha| = \alpha$  and  $|\mathcal{V}^\beta| = \beta$ . Say, for some  $\hat{v} \in \mathcal{V}^\alpha$ , that  $\hat{r}$  is the only connected request, that is,  $(\hat{r}, \hat{v}) \in \mathcal{E}$ . We know that the constraint  $Q_{\hat{r}} x_{\hat{r}\hat{v}} \leq \bar{Q}_{\hat{v}}$  cannot be active since its given  $Q_{\hat{r}} \leq \bar{Q}_{\hat{v}}$ , and by assumption  $0 < x_{\hat{r}\hat{v}} < 1$ . Hence,  $\forall v \in \mathcal{V}^\alpha$ , the corresponding constraint in  $\mathcal{C}_{\mathcal{V}}$  cannot be active. In addition to these constraints in  $\mathcal{C}_{\mathcal{V}}$ , the non-negativity constraints in (5) are also not active, which gives us the inequality

$$|\mathcal{R}| + |\mathcal{V}| - \alpha \geq |\mathcal{E}|, \quad (7)$$

because only a maximum of  $|\mathcal{R}| + |\mathcal{V}| - \alpha$  constraints can be active at  $\mathbf{x}$ . Now, from (6) and (7) we have

$$|\mathcal{R}| + |\mathcal{V}| - \alpha \geq |\mathcal{R}| + \frac{1}{2} \sum_{v \in \mathcal{V}} \deg(v) \quad (8)$$

$$\implies |\mathcal{V}| - \alpha \geq \frac{1}{2} \sum_{v \in \mathcal{V}^\alpha} \deg(v) + \frac{1}{2} \sum_{v \in \mathcal{V}^\beta} \deg(v) \quad (9)$$

$$= \frac{\alpha}{2} + \frac{1}{2} \sum_{v \in \mathcal{V}^\beta} \deg(v) \quad (10)$$

$$\implies \beta \geq \frac{\alpha}{2} + \frac{1}{2} \sum_{v \in \mathcal{V}^\beta} \deg(v) \geq \frac{\alpha}{2} + \beta. \quad (11)$$

From (11) we see that  $\alpha = 0$ , which together with (6) implies

$$|\mathcal{E}| \geq |\mathcal{R}| + |\mathcal{V}|. \quad (12)$$

In other words, all the constraints in  $\mathcal{C}_{\mathcal{R}}$  and  $\mathcal{C}_{\mathcal{V}}$  must be active. In order to complete the proof, it suffices to show that the constraints in  $\mathcal{C}_{\mathcal{R}}$  and  $\mathcal{C}_{\mathcal{V}}$  together are linearly dependent. Let  $\mathbf{A}$  be the constraint matrix of  $\text{LP}(G)$ , where  $\mathbf{a}_r$  is the row of  $\mathbf{A}$  corresponding to request  $r$  in  $\mathcal{C}_{\mathcal{R}}$  and  $\mathbf{a}_v$  is the row corresponding to vehicle  $v$  in  $\mathcal{C}_{\mathcal{V}}$ . We have that  $\sum_{r \in \mathcal{R}} Q_r \mathbf{a}_r = \sum_{v \in \mathcal{V}} \mathbf{a}_v$ ; in other words, the maximum number of linearly independent constraints that can be active at  $\mathbf{x}$  is strictly lower than  $|\mathcal{R}| + |\mathcal{V}|$ , thereby arriving at the required contradiction.  $\square$

### 3.4 Addressing $\text{LP}(G)$ infeasibility

It can happen that  $\text{LP}(G)$  is infeasible in an iteration of the IA; that is, given the set of requests  $\mathcal{R}$  and the set of vehicles  $\mathcal{V}$ , there does not exist an assignment that assigns all the requests in  $\mathcal{R}$ . One can easily see this happening when, for example, two requests  $r^1$  and  $r^2$  with  $Q_{r^1} = Q_{r^2} = 1$  and  $\deg(r^1) = \deg(r^2) = 1$  have  $v^0$  as the only feasible vehicle for both  $r^1$  and  $r^2$  with  $\bar{Q}_{v^0} = 1$ .



---

**Algorithm 2:  $G$  Reduction**


---

```

1 Inputs:  $\mathcal{R}, \mathcal{V}, \mathcal{E}, \mathcal{M}$ 
2  $\mathcal{R}^{\geq 2} \leftarrow \{r \in \mathcal{R} : Q_r \geq 2\}$ 
3 Order  $\mathcal{R}^{\geq 2}$  in the decreasing order of  $Q_r$ 
4 for  $r^0 \in \mathcal{R}^{\geq 2}$  do
5   if  $\exists v \in \mathcal{V} : (r^0, v) \in \mathcal{E}$  then
6      $v^0 \leftarrow \arg \min_{v \in \mathcal{V}} \{T_{r^0 v} : (r^0, v) \in \mathcal{E}\}$ 
7      $\mathcal{M} \leftarrow \mathcal{M} \cup \{(r^0, v^0)\}; \mathcal{R} \leftarrow \mathcal{R} \setminus \{r^0\}; \bar{Q}_{v^0} \leftarrow \bar{Q}_{v^0} - Q_{r^0}; \Theta_{v^0}^0 \leftarrow \Theta_{v^0}^{r^0}$ 
8      $\mathcal{E} \leftarrow \mathcal{E} \setminus \{(r^0, v) : v \in \mathcal{V}, (r^0, v) \in \mathcal{E}\}$ 
9     for  $r \in \mathcal{R} : (r, v^0) \in \mathcal{E}$  do
10      if edge  $(r, v^0)$  is infeasible then
11         $\mathcal{E} \leftarrow \mathcal{E} \setminus \{(r, v^0)\}$ 
12      else
13         $\text{Recompute } T_{rv^0}$ 
14  $\mathcal{R} \leftarrow \{r \in \mathcal{R} : \deg(r) \neq 0\}; \mathcal{V} \leftarrow \{v \in \mathcal{V} : \deg(v) \neq 0\}$ 
15  $G_U \leftarrow (\mathcal{R} \cup \mathcal{V}, \mathcal{E})$ 
16 return  $\mathcal{R}, \mathcal{V}, \mathcal{E}, G_U, \mathcal{M}$ 

```

---

When  $\text{LP}(G)$  is infeasible, instead of declaring infeasibility and leaving all the requests in  $\mathcal{R}$  unassigned or making an entirely greedy assignment in the iteration, we can conduct an informed assignment by making use of the structure of the polytope defined by the constraints of  $\text{LP}(G)$ . Consider greedily assigning, in the decreasing order of  $Q_r$ , requests with  $Q_r \geq 2$ . For a request  $r^0 \in \mathcal{R} : Q_{r^0} \geq 2$ , we assign vehicle  $v^0$  such that  $v^0 = \arg \min_{v \in \mathcal{V}} \{T_{r^0 v} : (r^0, v) \in \mathcal{E}\}$ , and we add the assignment to the matching  $\mathcal{M}$  that is returned when [Algorithm 1](#) terminates. Next we update  $v^0$ 's capacity and route plan, namely,  $\Theta_{v^0}^0 \leftarrow \Theta_{v^0}^{r^0}$ , after which  $\forall r \in \mathcal{R} : (r, v^0) \in \mathcal{E}$ , edge  $(r, v^0)$  is removed from  $\mathcal{E}$  if it is infeasible as per the capacity and delay thresholds; otherwise the cost of assignment  $T_{rv^0}$  is recomputed. If any request with  $Q_r \geq 2$  is left unassigned with no feasible vehicles, that request is removed from  $\mathcal{R}$  since it cannot be assigned in the current batch. After this process has completed,  $G$  that remains contains only those requests with  $Q_r = 1$ . This makes  $\text{LP}(G)$  the well-studied linear assignment problem on an integral polytope: the constraint matrix is totally unimodular, and the right-hand-side constraint vector is integral. We will refer to such a graph  $G$  as  $G_U$ , and we have that  $\text{LP}(G_U)$ , if feasible, returns an integral optimal extreme point solution. [Algorithm 2](#) formally states the procedure to reduce  $G$  to  $G_U$ . At this stage we do not know whether  $\text{LP}(G_U)$  is feasible or not; and as we will see, we do not require that piece of information. Consider the following linear program  $\bar{\text{LP}}(G_U)$  defined on  $G_U$ :

$$\bar{\text{LP}}(G_U) := \begin{cases} \text{maximize}_{x_{rv}} & \sum_{(r,v) \in \mathcal{E}} (M - T_{rv}) x_{rv} & (13) \\ \text{subject to} & \sum_{v: (r,v) \in \mathcal{E}} x_{rv} \leq 1, \forall r \in \mathcal{R} & (14) \\ & \sum_{r: (r,v) \in \mathcal{E}} x_{rv} \leq \bar{Q}_v, \forall v \in \mathcal{V} & (15) \\ & x_{rv} \geq 0, \forall (r, v) \in \mathcal{E}, & (16) \end{cases}$$

where  $M$  in (13) is a large enough positive value such that  $(M - T_{rv}) > 0, \forall (r, v) \in \mathcal{E}$ . We have that  $\bar{\text{LP}}(G_U)$  is a maximization problem with all positive costs, with the constraints  $\mathcal{C}_{\mathcal{R}}$  in (14)

being inequalities compared with equalities in (3). Since  $x_{rv} = 0, \forall (r, v) \in \mathcal{E}$  is a feasible solution to  $\overline{\text{LP}}(G_U)$ , we have that  $\overline{\text{LP}}(G_U)$  is always feasible. Even when  $\text{LP}(G_U)$  is infeasible,  $\overline{\text{LP}}(G_U)$  will make an informed potential assignment as the LP solution, which is then handled as usual within the IA. For cases where  $\text{LP}(G_U)$  is feasible, Lemma 2 tells us that with a carefully selected value for  $M$ , the optimal solution returned by  $\overline{\text{LP}}(G_U)$  is optimal for  $\text{LP}(G_U)$  as well. Hence, in an iteration of the IA where it has been identified that  $\text{LP}(G)$  is infeasible, we first reduce  $G$  to  $G_U$  by greedily assigning requests with  $Q_r \geq 2$ , and then we proceed to solve  $\overline{\text{LP}}(G_U)$ .

**Lemma 2.** *If  $\text{LP}(G_U)$  is feasible,  $\exists M < \infty$  such that  $\bar{\mathbf{x}}^*$  optimal for  $\overline{\text{LP}}(G_U)$  is also optimal for  $\text{LP}(G_U)$ .*

*Proof.* Let  $\mathcal{P}$  and  $\overline{\mathcal{P}}$  be the polytopes defined by the constraints of  $\text{LP}(G_U)$  and  $\overline{\text{LP}}(G_U)$ , respectively. Let  $\mathbf{x}^*$  and  $\bar{\mathbf{x}}^*$  be optimal extreme point solutions to  $\text{LP}(G_U)$  and  $\overline{\text{LP}}(G_U)$ , respectively. We have that  $\mathbf{x}^* \in \overline{\mathcal{P}}$ , since  $\mathcal{P} \subseteq \overline{\mathcal{P}}$  because constraints  $\mathcal{C}_{\mathcal{R}}$  in (14) are relaxed versions of those in (3). Let  $f(\mathbf{x})$  and  $\bar{f}(\mathbf{x})$  be the objective function of  $\text{LP}(G_U)$  and  $\overline{\text{LP}}(G_U)$ , respectively. We have

$$\bar{f}(\bar{\mathbf{x}}^*) \geq \bar{f}(\mathbf{x}^*) \quad (17)$$

$$\implies \sum_{(r,v) \in \mathcal{E}} (M - T_{rv}) \bar{x}_{rv}^* \geq \sum_{(r,v) \in \mathcal{E}} (M - T_{rv}) x_{rv}^* \quad (18)$$

$$\implies M \sum_{(r,v) \in \mathcal{E}} (\bar{x}_{rv}^* - x_{rv}^*) \geq \sum_{(r,v) \in \mathcal{E}} T_{rv} (\bar{x}_{rv}^* - x_{rv}^*) \quad (19)$$

$$= f(\bar{\mathbf{x}}^*) - f(\mathbf{x}^*). \quad (20)$$

The equality constraints in (3) imply that  $\sum_{(r,v) \in \mathcal{E}} x_{rv}^* = |\mathcal{R}|$ , so that we get

$$M \left( \sum_{(r,v) \in \mathcal{E}} \bar{x}_{rv}^* - |\mathcal{R}| \right) \geq f(\bar{\mathbf{x}}^*) - f(\mathbf{x}^*) \quad (21)$$

$$\implies \sum_{(r,v) \in \mathcal{E}} \bar{x}_{rv}^* \geq |\mathcal{R}| - \frac{(f(\mathbf{x}^*) - f(\bar{\mathbf{x}}^*))}{M}. \quad (22)$$

The constraints  $\mathcal{C}_{\mathcal{R}}$  in (14) imply that  $\sum_{(r,v) \in \mathcal{E}} \bar{x}_{rv}^* \leq |\mathcal{R}|$ , and together with (22) we have that  $f(\mathbf{x}^*) - f(\bar{\mathbf{x}}^*) \geq 0$ . Now, if we select a value for  $M$  such that it is guaranteed that  $M > f(\mathbf{x}^*) - f(\bar{\mathbf{x}}^*)$ , then we have  $\sum_{(r,v) \in \mathcal{E}} \bar{x}_{rv}^* = |\mathcal{R}|$  since  $\overline{\text{LP}}(G_U)$  returns an integral optimal extreme point solution. When  $\sum_{(r,v) \in \mathcal{E}} \bar{x}_{rv}^* = |\mathcal{R}|$ , we have that  $\bar{\mathbf{x}}^* \in \mathcal{P}$ ; and equation (21) implies that  $f(\bar{\mathbf{x}}^*) \leq f(\mathbf{x}^*)$ , which means  $\bar{\mathbf{x}}^*$  is optimal for  $\text{LP}(G_U)$ . Now it remains to identify a suitable value for  $M$  in order to complete the proof. We know that the minimum value  $f(\bar{\mathbf{x}}^*)$  can possibly take is 0 and that the maximum value  $f(\mathbf{x}^*)$  can take is  $\sum_{r \in \mathcal{R}} \max\{T_{rv} : (r, v) \in \mathcal{E}\}$ . Hence, if we set  $M = \left( \sum_{r \in \mathcal{R}} \max\{T_{rv} : (r, v) \in \mathcal{E}\} \right) + \epsilon$ , where  $\epsilon > 0$ , then  $\bar{\mathbf{x}}^*$  that is optimal for  $\overline{\text{LP}}(G_U)$  is also optimal for  $\text{LP}(G_U)$ .  $\square$

### 3.5 Fleet operator and customer perspective

The travel time optimization in  $\text{LP}(G)$  uses  $T_{rv}$  as the cost, minimizing which translates to reducing the overall travel times for the fleet and hence is an optimization from the fleet operator's perspective. This might lead to larger travel times for the customers since the optimization in essence tries

to enhance ridesharing, often at the expense of delay to the customers. A straightforward approach to account for customer delays in the optimization is to add a customer-centric cost component to the optimization. Similar to  $T_{rv}$ ,  $\forall (r, v) \in \mathcal{E}$  we define  $W_{rv}$  to be the maximum delay of all customers served by vehicle  $v$  on the potential route plan  $\Theta_v^r$ . The delay for a request is calculated as the difference between its expected travel time without ridesharing and the sum of travel time and pick-up time on the potential route plan. Now, instead of  $T_{rv}$  as the cost, we could use a convex combination of  $T_{rv}$  and  $W_{rv}$  as the new cost, that is, define the cost of assigning  $r$  to  $v$  as

$$\tilde{T}_{rv} := \Lambda T_{rv} + (1 - \Lambda)W_{rv}, \quad (23)$$

where  $\Lambda$  is a scaling parameter in the interval  $[0, 1]$ . Here, the optimization is fleet operator-centric when  $\Lambda$  is closer to 1 and customer-centric when  $\Lambda$  is closer to 0.

### 3.6 Greedy real-time assignment

We will show that the IA algorithm efficiently solves dynamic ridesharing problems considered. We will also consider a simpler “greedy” approach to dynamic ridesharing to compare the trade-off between the solution quality and computational time. This greedy procedure, derived from the heuristic in (Gurumurthy et al., 2020) and summarized in Algorithm 3, is executed each time a request appears. First, it seeks to assign requests to nearby vehicles while attempting to ensure all assigned requests are picked up within the predefined threshold. When a request comes in, the algorithm finds the nearest feasible vehicle: a vehicle that could complete the new request and all other requests it is already serving, within the threshold pick-up times. (This calculation of pick-up time uses Euclidean leg distances and an average zone-based speed updated every hour to avoid computationally intensive router calls.) Second, Algorithm 3 seeks to assign requests to in-progress trips that are going in the same direction. This is accomplished by comparing the angle between a vehicle’s current position to its destination and the vehicle’s current position to the new request’s destination. If this angle is sufficiently small (in experiments we use a threshold of 10 degrees), the vehicle is selected for matching. Once the match is made, all ongoing pick-ups and drop-offs for a vehicle are reordered using the heuristic nearest-neighbor search while constraining travelers to be dropped off only after they are picked up.

Once a trip has been assigned, a series of delay checks occur: at the end of each pick-up or drop-off operation, all travelers’ current delay is verified. If any traveler is close to experiencing a delay greater than  $D_r^T$ , that vehicle stops accepting requests and does not show up in other queries until all passengers have been dropped off. While this is computationally beneficial, it does not provide a clear upper bound on  $D_r^T$  but instead only limits passenger delays from being unbounded.

Previous uses of this greedy approach (Gurumurthy et al., 2021; Gurumurthy and Kockelman, 2022) have shown to improve average vehicle occupancy and fleet efficiency and help decrease system-wide vehicle miles traveled. By comparing the proposed method in this study to a benchmark implemented within the same simulation framework (POLARIS), we will show that the IA efficiently solves large-scale dynamic ridesharing problem instances.

---

**Algorithm 3:** Greedy real-time assignment for a given request  $r$ 

---

```
1 while  $r$  not assigned do
2   Query nearest vehicle  $v$  to the request's origin  $r^o$ 
3   if  $v$  is idle then
4     Assign  $r$  to  $v$ 
5   else
6     if  $v$  has seats available then
7       Let  $v^{pos}$  be  $v$ 's current location and  $v^d$  be its final destination
8       if The angle between directions  $v^{pos} \rightarrow v^d$  and  $v^{pos} \rightarrow r^d$  is small then
9         if  $r$  and its already assigned travelers can be picked up within pick-up threshold  $D^P$  then
10          Assign  $r$  to  $v$ 
11         else
12           Exclude  $v$  from future nearest vehicle query for  $r$ 
13       else
14         Exclude  $v$  from future nearest vehicle query for  $r$ 
15     else
16       Exclude  $v$  from future nearest vehicle query for  $r$ 
```

---

## 4 Numerical Experiments

In this section we carry out multiple experiments on a POLARIS model of the city of Austin, Texas, United States. We compare the IA with the greedy approach, then study the effect of fleet size and key parameters.

### 4.1 Scenario setting

We focus our study on the areas closer to the city of Austin and its downtown area where the requests are concentrated. Figure [Figure 1](#) shows the Austin network. The light gray area depicts the excluded zones while the green area shows the zones included in the geofence. This network contains more than 40K links and 17K nodes. The network used is based on the local Capital Area Metropolitan Planning Organization (CAMPO) and comprises a large area containing 8 counties.

We generate the demand following the POLARIS agent-based modeling framework. The demand is an outcome of the population synthesis and its travel decisions throughout the day. The model's agents decide what activity they will do each day (work, shopping, personal, etc.) and for how long, as well as where they will do it. Based on the activity plan, agents then decide departure times and modes based on the expected travel times for each mode and their availability. Model parameters are calibrated to match the observed outcomes regarding mode shares, trip distances, departure time distributions, and the number of activities performed. We refer to the appendix in [Dean et al. \(2022\)](#) for a comparison between the simulated and observed metrics in the CAMPO area.

For this study we recorded all the TNC/taxi trips in the target area and kept the same request pattern for all the simulations. This corresponds to 153,323 requests in a 24-hour period. We also keep the same set of trips of 4.5M single-occupant vehicles as background traffic. We run all simulations with a traffic time step of 2 seconds.

Unless otherwise stated, the batching period  $B$  is 30 seconds; the number of potential to consider  $N$  is 10% of the fleet size; the objective weight  $\Lambda$  is 0.5; and the maximum allowed pick-up delay for any request  $D^P$  and the maximum allowed travel delay  $D_r^T$  are 30 minutes. These are relatively high maximum allowable delays, but we keep these values because they were used for the greedy

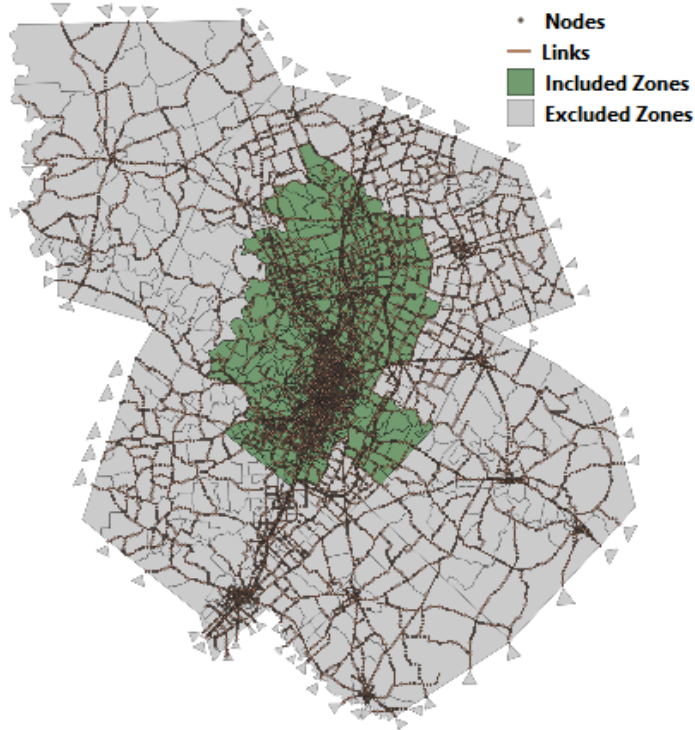


Figure 1: Austin network.

approach when calibrating the model. Moreover, the results will show that the average delays are typically much smaller than the maximum delays.

## 4.2 Fleet size comparison with the greedy assignment

In the first set of experiments, we compare the outcomes of the proposed iterative scheme with the greedy approach for different fleet sizes ranging from 1,500 to 3,000 vehicles.

Figure 2 depicts the total VHT (left), the share of requests served (middle), and the wait times (right) for the greedy (blue) and the IA (orange) for different fleet sizes. The IA yields lower VHT for all fleet sizes with a marginally higher share of requests served. The only exception is the fleet size of 3,000 vehicles in which the greedy method serves a slightly higher number of requests. Conversely, the greedy approach can keep lower wait times for all cases.

The complete set of metrics is reported in Table 2. The fleet size denotes the number of vehicles. The greedy approach yields lower wait and journey times, which is an outcome of its behavior of (i) assigning requests generally to the closest available vehicle, which leads to lower waiting times. and (ii) because the closest vehicle is often not a suitable match for pooling, which leads to lower journey time. However, it requires more travel per request on average and serves slightly fewer requests for lower fleet sizes. The IA processes 30-second batches in less than half a second on average. This result proves that the method is efficient and suitable for real-time use in this scenario. Note that CPU time is not reported for the greedy approach: thbatching interval concept is not needed for the greedy approach and the CPU time is negligible because the method can be as quick as retrieving the closest vehicle from a double-ended queue (in the best case) and checking multiple

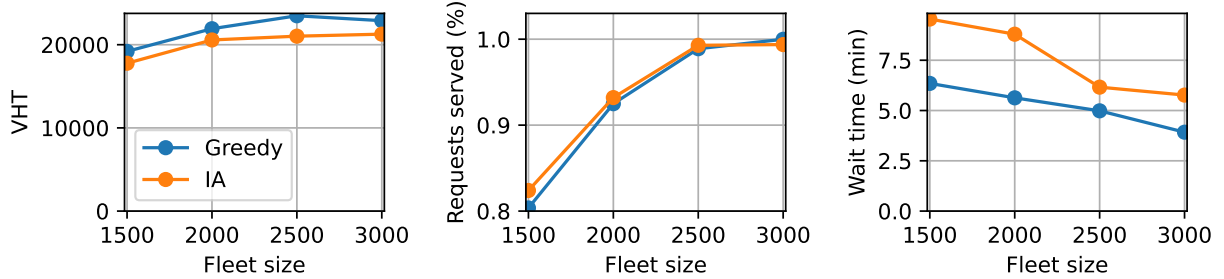


Figure 2: Comparison between the IA and the greedy approach for different fleet sizes.

vehicles (in the worst case).

Fleet size	Strategy	Served (%)	Travel per req. (min)	Journey time (min)	Wait time (min)	CPU (s)
1,500	Greedy	80.36	9.36	20.94	6.35	
	IA	82.40	8.44	25.44	9.54	0.39
	$\Delta\%$	+2.04	-9.82	+21.48	+50.23	
2,000	Greedy	92.49	9.28	19.56	5.63	
	IA	93.20	8.64	24.58	8.70	0.36
	$\Delta\%$	+0.71	-6.89	+25.66	+54.52	
2,500	Greedy	98.89	9.30	18.06	4.98	
	IA	99.29	8.29	19.32	6.16	0.35
	$\Delta\%$	+0.40	-10.86	+6.97	23.69	
3,000	Greedy	99.99	8.96	15.81	3.92	
	IA	99.37	8.38	18.64	5.76	0.36
	$\Delta\%$	-0.62	-6.47	+17.90	+46.93	

Table 2: Key metrics for different fleet sizes using the IA and the greedy approach.

The reason for the higher wait time on the IA is that it maintains a higher vehicle occupancy than does the greedy approach. By increasing pooling with requests with fewer detours, the IA can reduce the total VHT at the expense of higher wait times. This pattern is clearer in assessing the time-series comparison. Figure 3 depicts average occupancy (left), time spent on the network (middle), and average wait time (right) over the 24-hour period. Outside the peak, the proposed IA strategy consistently keeps higher vehicle occupancy. This results in slightly slower time spent in the network, higher wait time, and lower fleet size to serve the same demand.

The key performance distinction occurs during the peak period. One can observe in the left graph in Figure 3 that the occupancy for both strategies spikes at around 7AM. The greedy strategy keeps the occupancy around 1.5 until noon, whereas the IA exceeds two people per vehicle. This results in an overall fewer vehicles used and therefore less time spent in the network over that period, which is clear in the middle graph. The IA strategy serves the same amount of requests while yielding approximately 8% less VHT (see Figure 2).

The IA strategy is aware of the need to increase pooling when there are fewer vehicles, as evidenced by the vehicle occupancy for different fleet sizes. Figure 3 depicts the same metrics (occupancy, time spent, and wait time from left to right) for the IA strategy for four different fleet

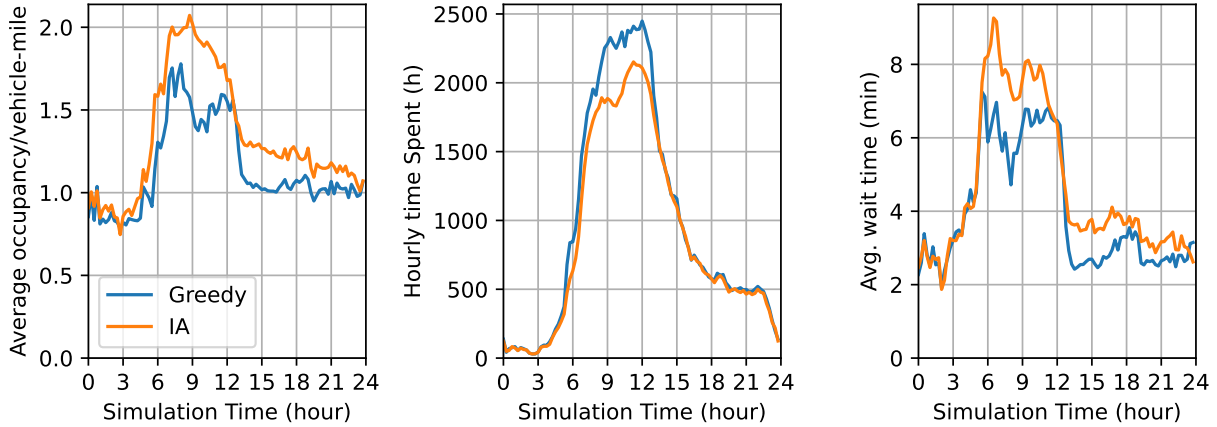


Figure 3: Temporal comparison between the IA and the greedy approach for 2,500 -vehicle case.

sizes. The average occupancy decreases following the peak earlier, the higher the fleet size is. The reduction in occupancy results in lower wait time and higher time spent during that period.

### 4.3 Effect of the number of vehicles considered per request

The IA strategy takes  $N$ , the number of potential vehicles to consider for each request, as an input parameter. Reducing  $N$  saves computational time as it potentially decreases the number of decision variables in the optimization problem and the number of routes to be computed. On the other hand, a higher number of vehicles per request gives more flexibility to the solver to find better solutions. In this section we assess the trade-offs for  $N$  by assessing the results for  $N \in \{125, 250, 500\}$  for a fleet of 2,500 vehicles.

Figure 4 shows the VHT (left), the share of requests served (middle), and the average wait time (right) for the three different fleet sizes. For all three metrics, the performance changes are marginal. Increasing  $N$  leads to more requests served and lower wait time, although the total VHT is slightly higher for bigger  $N$ . In terms of VHT per request, the results are also favorable for the  $N = 500$  case since it served more requests.

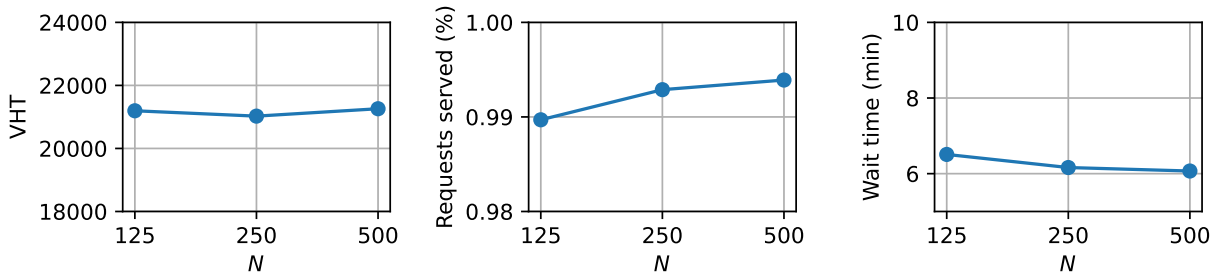


Figure 4: VHT (left), share of requests served (middle), and average wait time (right) as a function of vehicles considered per request ( $N$ ).

Table 3 provides further insights for this analysis. Even though travel per request goes up with

$N = 500$ , this case has the shortest journey and wait time compared with other cases. As expected, the CPU time increases for higher  $N$ . Nevertheless, the average CPU time is still low enough for real-time operation for batches of 30 seconds for this scenario.

Fleet size	$N$	Served (%)	Travel per req. (min)	Journey time (min)	Wait time (min)	CPU time (s)
2,500	125	98.97	8.39	20.64	6.50	0.16
	250	99.29	8.29	19.32	6.16	0.35
	500	99.39	8.38	18.81	6.07	0.54

Table 3: Key metrics for vehicles per request using the IA strategy.

#### 4.4 Effect of objective function weight

We perform a similar comparison for the objective function parameter  $\Lambda$  that weights between service- ( $\Lambda \rightarrow 1$ ) and customer ( $\Lambda \rightarrow 0$ )-centric operation. To that end, we perform experiments for  $\Lambda \in \{0.25, 0.5, 0.75\}$ .

For this parameter sensitivity, the results are salient. Figure 5 shows the VHT (left), the share of requests served (middle), and the average wait time (right) for the three values of  $\Lambda$ . Increasing  $\Lambda$  leads to a significant decrease in the total VHT. On the other hand, there is a decrease in the number of requests served, and the wait time for the case of  $\Lambda = 0.75$  is around 10% higher than the other two values of  $\Lambda$ .

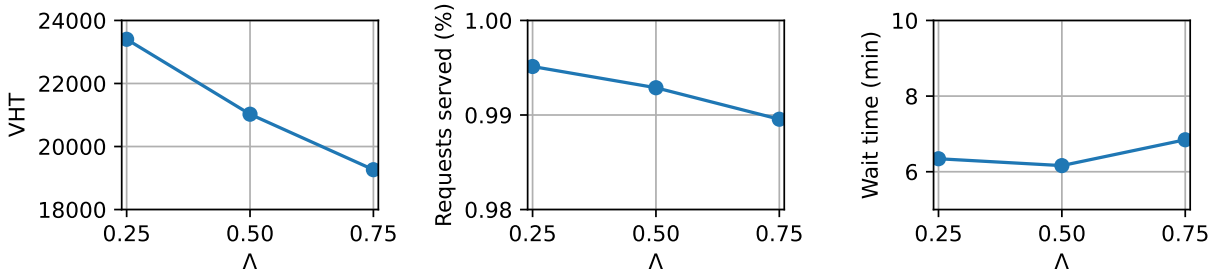


Figure 5: VHT (left), share of requests served (middle), and average wait time (right) as function of objective function weight  $\Lambda$ .

The reason behind the changes in the VHT for higher values of  $\Lambda$  is the higher amount of pooling achieved in these cases. This is clear in the temporal evolution of vehicle occupancy (left), time spent in the network (middle), and average wait time (right) in Figure 6. The average occupancy is substantially higher values of  $\Lambda$ , which in turn leads to lower VHT. Nevertheless, the average occupancy for  $\Lambda = 0.5$  is smaller than the the average occupancy for  $\Lambda = 0.75$ , but that does not lead to significant changes in VHT during the peak period. On the other hand, the  $\Lambda = 0.25$  case leads to a significantly higher VHT at that period.

Table 4 presents the share of served requests, travel time per request, and journey, wait, and CPU times for the three different values of  $\Lambda$ .



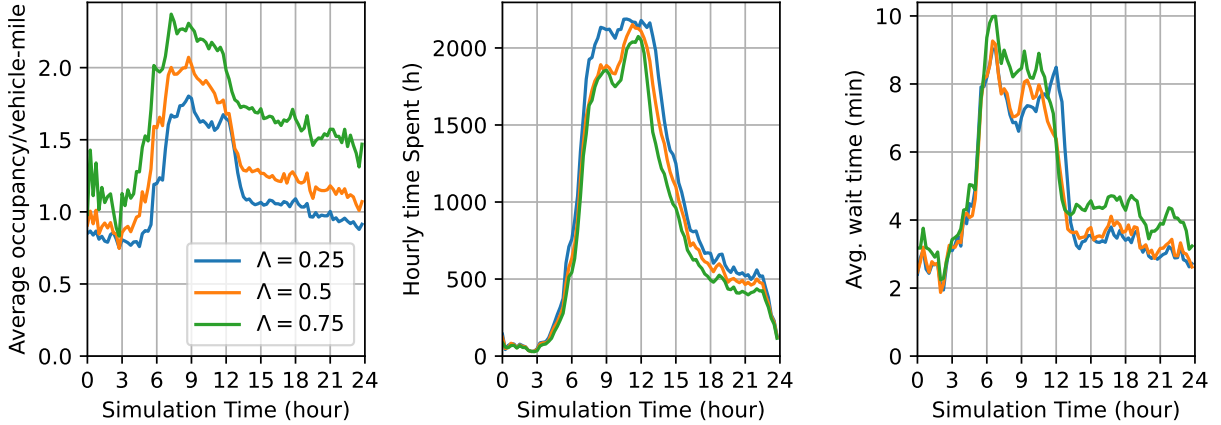


Figure 6: Average occupancy (left), hourly time spent (middle), and average wait time (right) for  $\Lambda \in \{0.25, 0.5, 0.75\}$

Fleet size	$\Lambda$	Served (%)	Travel per req. (min)	Journey time (min)	Wait time (min)	CPU time (s)
2,500	0.25	99.51	9.21	19.03	6.34	0.36
	0.50	99.29	8.29	19.32	6.16	0.35
	0.75	98.96	7.62	21.62	6.84	0.32

Table 4: Key metrics for vehicles per request using the IA strategy for different  $\Lambda$  values.

#### 4.5 Effect of the batching interval

The batching interval  $B$  has a potential impact on the solution quality. It does not influence the modeling; however, the set of requests for each batch is dependent upon  $B$ . A shorter batching interval means that each request is processed earlier, and it can lead to lower wait times for the same assignment set. On the other hand, the solver is provided less flexibility for making decisions and therefore may make worse decisions. In this study we test  $B \in \{15, 30, 60\}$  seconds.

Figure 7 shows the VHT (left), share of requests served (right), and average waiting time (right). Overall, the batching interval is the lever with the least variations in outcome. Nevertheless, there are interesting aspects to it. Increasing the batching interval leads to a VHT decrease, which was expected. However, the change in wait time is marginal and much lower than the average time for processing the batch (half of the batching interval). Therefore, the highest batching intervals would be advised in this particular case.

Table 5 shows the share of served vehicles, travel per request, journey time, wait time, and CPU time for different batching intervals. The table also supports that  $B$  does not have a considerable impact on the key performance metrics, yet it plays a critical role in the CPU time.

## 5 Conclusion

The DRS is a challenging problem due to the impact of service order complexity on the system performance. Moreover, the two parties involved in the problem—riders and operators—pursue different objectives. In this study we developed an optimization model considering a balanced

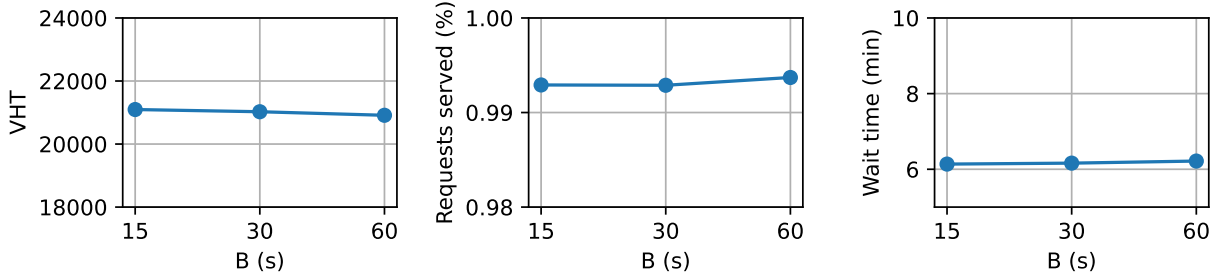


Figure 7: VHT (left), share of requests served (middle), and average wait time (right) as function of batching interval (B).

Fleet size	$B$	Served (%)	Travel per req. (min)	Journey time (min)	Wait time (min)	CPU time (s)
2,500	15	99.29	8.32	19.39	6.16	0.16
	30	99.29	8.29	19.32	6.16	0.35
	60	99.37	8.24	19.11	6.21	0.80

Table 5: Key metrics for vehicles per request using the IA strategy for different batching interval.

objective to solve the DRS problem. In this problem, time-to-solution is one of the key performance metrics because vehicle assignments need to be handled quickly to satisfy riders. To this end, we proposed the IA approach for the DRS problem. The problem is cast in a series of linear programs to assign riders to vehicles. We prove the optimality of the approach even in the case of multiple party sizes. Moreover, the method is computationally efficient since it relies on linear programming. As a benchmark, we develop a greedy heuristic solution and compare the computational performance and key solution quality metrics. The IA implementation compared with the greedy method in Austin, TX, showed shorter journey time and wait time with the expense of CPU time increase.

In the studies around key parameters, we found the objective function weight is the most significant in changing the outcomes. A service-centric objective leads to lower VHT at the expense of higher average wait times. The batching interval and the number of vehicles per request have some impacts, but they are limited. The key mechanism for the different outcomes in the objective function is the average occupancy. A higher weight  $\Lambda$  on the total travel time induces more pooling, which reduces VHT and increases wait and journey times.

In this study we did not consider repositioning of the vehicles. In a DRS network, the distribution of vehicles can impact the overall service quality. One may target repositioning a vehicle from its low-demand last service destination to a high-demand destination to increase the probability of a better match. While this unoccupied travel incurs cost and time, it may increase customer satisfaction with faster service. The DRS problem could incorporate repositioning decisions while making assignments.

Fossil fuel vehicles leave a large footprint on the environment, and governments now have global goals toward net-zero emissions. Vehicle electrification is a top priority among actions toward achieving these goals. In this study we did not schedule charging activities, which is a challenging task and adds to the complexity of the DRS problem. Future studies should consider these aspects to address the electrification in this industry.

## **Acknowledgments**

This material is based upon work supported by the U.S. Department of Energy, Office of Science, under contract number DE-AC02-06CH11357. This report and the work described were sponsored by the U.S. Department of Energy (DOE) Vehicle Technologies Office (VTO) under the Systems and Modeling for Accelerated Research in Transportation (SMART) Mobility Laboratory Consortium, an initiative of the Energy Efficient Mobility Systems (EEMS) Program. Erin Boyd, a DOE Office of Energy Efficiency and Renewable Energy (EERE) manager, played an important role in establishing the project concept, advancing implementation, and providing guidance. The authors remain responsible for all findings and opinions presented in the paper. The findings are not suggestions for agencies to implement given the assumptions made in this study.

## References

- Agatz, N., Erera, A., Savelsbergh, M., Wang, X., 2012. Optimization for dynamic ride-sharing: A review. *European Journal of Operational Research* 223, 295–303. doi:[10.1016/j.ejor.2012.05.028](https://doi.org/10.1016/j.ejor.2012.05.028).
- Agatz, N.A., Erera, A.L., Savelsbergh, M.W., Wang, X., 2011. Dynamic ride-sharing: A simulation study in metro Atlanta. *Transportation Research Part B: Methodological* 45, 1450–1464. doi:[10.1016/j.trb.2011.05.017](https://doi.org/10.1016/j.trb.2011.05.017).
- Aissi, H., Bazgan, C., Vanderpooten, D., 2008. Complexity of the min–max (regret) versions of min cut problems. *Discrete Optimization* 5, 66–73. doi:[10.1016/j.disopt.2007.11.008](https://doi.org/10.1016/j.disopt.2007.11.008).
- Alisoltani, N., Leclercq, L., Zargayouna, M., 2021. Can dynamic ride-sharing reduce traffic congestion? *Transportation Research Part B: Methodological* 145, 212–246. doi:[10.1016/j.trb.2021.01.004](https://doi.org/10.1016/j.trb.2021.01.004).
- Alonso-Mora, J., Samaranayake, S., Wallar, A., Frazzoli, E., Rus, D., 2017. On-demand high-capacity ride-sharing via dynamic trip-vehicle assignment. *Proceedings of the National Academy of Sciences* 114, 462–467. doi:[10.1073/pnas.1611675114](https://doi.org/10.1073/pnas.1611675114).
- Auld, J., Hope, M., Ley, H., Sokolov, V., Xu, B., Zhang, K., 2016. POLARIS: Agent-based modeling framework development and implementation for integrated travel demand and network and operations simulations. *Transportation Research Part C: Emerging Technologies* 64, 101–116. doi:[10.1016/j.trc.2015.07.017](https://doi.org/10.1016/j.trc.2015.07.017).
- Dean, M.D., Gurumurthy, K.M., de Souza, F., Auld, J., Kockelman, K.M., 2022. Synergies between repositioning and charging strategies for shared autonomous electric vehicle fleets. *Transportation Research Part D: Transport and Environment* 108, 103314. doi:[10.1016/j.trd.2022.103314](https://doi.org/10.1016/j.trd.2022.103314).
- Furuhata, M., Dessouky, M., Ordóñez, F., Brunet, M.E., Wang, X., Koenig, S., 2013. Ridesharing: The state-of-the-art and future directions. *Transportation Research Part B: Methodological* 57, 28–46. doi:[10.1016/j.trb.2013.08.012](https://doi.org/10.1016/j.trb.2013.08.012).
- Gurumurthy, K.M., Auld, J., Kockelman, K., 2021. A system of shared autonomous vehicles for Chicago: Understanding the effects of geofencing the service. *Journal of Transport and Land Use* 14, 933–948. doi:[10.5198/jtlu.2021.1926](https://doi.org/10.5198/jtlu.2021.1926).
- Gurumurthy, K.M., Kockelman, K.M., 2022. Dynamic ride-sharing impacts of greater trip demand and aggregation at stops in shared autonomous vehicle systems. *Transportation Research Part A: Policy and Practice* 160, 114–125. doi:[10.1016/j.tra.2022.03.032](https://doi.org/10.1016/j.tra.2022.03.032).
- Gurumurthy, K.M., de Souza, F., Enam, A., Auld, J., 2020. Integrating supply and demand perspectives for a large-scale simulation of shared autonomous vehicles. *Transportation Research Record: Journal of the Transportation Research Board* 2674, 181–192. doi:[10.1177/0361198120921157](https://doi.org/10.1177/0361198120921157).
- Johnson, E.L., Mehrotra, A., Nemhauser, G.L., 1993. Min-cut clustering. *Mathematical Programming* 62, 133–151. doi:[10.1007/BF01585164](https://doi.org/10.1007/BF01585164).
- Lau, L.C., Ravi, R., Singh, M., 2011. *Iterative Methods in Combinatorial Optimization*. Cambridge University Press. doi:[10.1017/cbo9780511977152](https://doi.org/10.1017/cbo9780511977152).

- Lawler, R., 2014. Uber opens up UberPool to all San Francisco users. TechCrunch URL: <https://techcrunch.com/2014/09/02/uberpool-launch-for-real/>.
- Martins, L.d.C., de la Torre, R., Corlu, C.G., Juan, A.A., Masmoudi, M.A., 2021. Optimizing ride-sharing operations in smart sustainable cities: Challenges and the need for agile algorithms. *Computers & Industrial Engineering* 153, 107080. doi:[10.1016/j.cie.2020.107080](https://doi.org/10.1016/j.cie.2020.107080).
- Masoud, N., Jayakrishnan, R., 2017a. A decomposition algorithm to solve the multi-hop peer-to-peer ride-matching problem. *Transportation Research Part B: Methodological* 99, 1–29. doi:[10.1016/j.trb.2017.01.004](https://doi.org/10.1016/j.trb.2017.01.004).
- Masoud, N., Jayakrishnan, R., 2017b. A real-time algorithm to solve the peer-to-peer ride-matching problem in a flexible ridesharing system. *Transportation Research Part B: Methodological* 106, 218–236. doi:[10.1016/j.trb.2017.10.006](https://doi.org/10.1016/j.trb.2017.10.006).
- Morency, C., 2007. The ambivalence of ridesharing. *Transportation* 34, 239–253. doi:[10.1007/s11116-006-9101-9](https://doi.org/10.1007/s11116-006-9101-9).
- Najmi, A., Rey, D., Rashidi, T.H., 2017. Novel dynamic formulations for real-time ride-sharing systems. *Transportation Research Part E: Logistics and Transportation Review* 108, 122–140. doi:[10.1016/j.tre.2017.10.009](https://doi.org/10.1016/j.tre.2017.10.009).
- Nourinejad, M., Roorda, M.J., 2016. Agent based model for dynamic ridesharing. *Transportation Research Part C: Emerging Technologies* 64, 117–132. doi:[10.1016/j.trc.2015.07.016](https://doi.org/10.1016/j.trc.2015.07.016).
- Pelzer, D., Xiao, J., Zehe, D., Lees, M.H., Knoll, A.C., Aydt, H., 2015. A partition-based match making algorithm for dynamic ridesharing. *IEEE Transactions on Intelligent Transportation Systems* 16, 2587–2598. doi:[10.1109/TITS.2015.2413453](https://doi.org/10.1109/TITS.2015.2413453).
- Sarriera, J.M., Álvarez, G.E., Blynn, K., Alesbury, A., Scully, T., Zhao, J., 2017. To share or not to share: Investigating the social aspects of dynamic ridesharing. *Transportation Research Record* 2605, 109–117. doi:[10.3141/2605-11](https://doi.org/10.3141/2605-11).
- Shen, B., Huang, Y., Zhao, Y., 2016. Dynamic ridesharing. *SIGSPATIAL Special* 7, 3–10. doi:[10.1145/2876480.2876483](https://doi.org/10.1145/2876480.2876483).
- Tafreshian, A., Masoud, N., Yin, Y., 2020. Frontiers in service science: Ride matching for peer-to-peer ride sharing: A review and future directions. *Service Science* 12, 44–60. doi:[10.1287/serv.2020.0258](https://doi.org/10.1287/serv.2020.0258).
- Tahmasseby, S., Kattan, L., Barbour, B., 2014. Dynamic real-time ridesharing: A literature review and early findings from a market demand study of a dynamic transportation trading platform for the University of Calgary’s main campus. *Transportation Research Board 93rd Annual Meeting* URL: <https://trid.trb.org/view/1288694>.

The submitted manuscript has been created by UChicago Argonne, LLC, Operator of Argonne National Laboratory (“Argonne”). Argonne, a U.S. Department of Energy Office of Science laboratory, is operated under Contract No. DE-AC02-06CH11357. The U.S. Government retains for itself, and others acting on its behalf, a paid-up nonexclusive, irrevocable worldwide license in said article to reproduce, prepare derivative works, distribute copies to the public, and perform publicly and display publicly, by or on behalf of the Government. The Department of Energy will provide public access to these results of federally sponsored research in accordance with the DOE Public Access Plan <http://energy.gov/downloads/doe-public-access-plan>.